Numerical modeling approach of an artificial mangrove root system (ArMS) submerged breakwater as wetland habitat protector

by Eldina Fatimah[1], Ahmad Khairi Abd. Wahab[2], and Hadibah Ismail[3]

ABSTRACT

An artificial mangrove root system was proposed as an alternative solution to solve coastal engineering problems in cohesive soil coastlines. Numerical modeling was carried out to determine the wave-structure interaction to provide information on the performance of the system. A commercial computational fluid dynamics software was applied to simulate the propagation of waves over the structure. The variables that were used in the numerical work are wave height (H_i), wave length (L), water depth (d), structure height (d_s), structure porosity (ζ), and structure width (W) for the 1-, 3-, 5-, and 20-row systems. These variables were analyzed in a non-dimensional form as relative wave steepness (H_i/L), relative water depth (d/L), relative structure height (d_s/d), and relative structure width (W/L). The influences of these parameters on the wave transmission (C_t), reflection (C_r) and energy dissipation (C_l) coefficients were studied. The accuracy of the numerical model was verified by comparing the numerical results with the experimental data. Comparison between numerical and experimental results on the wave transmission coefficients showed good agreement. For the range of 1- to 20-row systems that were tested, the numerical results revealed that C_t decreases from 0.95 to 0.13 as the porosity decreases from 0.95 to 0.75 for H_i/L = 0.005. The system is more effective in reducing wave energy at $d_s/d \geq 1.0$ and at $d/L \geq 0.15$.

1. INTRODUCTION

Nowadays there is a strong negative public reaction to the hard conventional rock emplacement along the coast. During the past 20 years, coastal structure are designed with so called “soft-methods” e.g. beach nourishment, submerged breakwaters, artificial reefs, gravity drain systems, floating breakwater, plantations of hydrophyle shrubs, dry benches, etc. Therefore with the recent trend to seek shoreline protection with low environmental impact, it is very challenging for the coastal engineer to innovatively design a new type of coastal protection structure which is suitable technically but at the same time be able to act-naturally to protect the mangrove seedling zone or wetland habitat and at the same time control shoreline erosion.

Porous submerged breakwaters have been extensively used in coastal zones for shoreline protection and to prevent beach erosion. The purpose of this kind of structure is to reduce the transmitted wave energy by reducing reflected waves and dissipating the incident wave energy by inciting wave breaking and increasing flow friction through the porous media.

Wave transformation over the porous structure is difficult to estimate, mainly due to the complexity of the porous structures and breaking wave conditions. Several researchers have presented a number of numerical models relating to this problem. Submerged wave filter which is integrated in multilayer systems of permeable vertical walls has been introduced by Clauss G. F and Habel R (1999) and fine mesh wave barrier was studied by Wang K. and Williams (2003) while Armono (1998) has investigated bottom-seated smooth-shaped artificial reef.

Taking the concept of ability of mangrove plants to convert the mean kinetic energy into turbulent kinetic energy, it is a challenging effort to investigate the effect of mangrove-roots-like submerged breakwater, known as ArMS (short for Artificial Mangrove Root System) on the hydraulic behavior. ArMS geometrics were basically designed by simplifying the complicated mangrove root systems into a simple and easy to construct porous submerged structure. The nature of these porous submerged structures was investigated and the results could be used as a technical guidance. This innovative

[1] Postgraduate student, Coastal and Offshore Engineering Institute/Faculty of Civil Engineering, Universiti Teknologi Malaysia, Email: Eldinafatimah@yahoo.com

[2] Associate Professor/ Director, Coastal and Offshore Engineering Institute, Universiti Teknologi Malaysia City Campus, Kuala Lumpur, Email:dr_khairi@citycampus.utm.my

[3] Professor/ Coastal and Offshore Engineering Institute, Universiti Teknologi Malaysia City Campus, Kuala Lumpur, Email: hadibah@citycampus.utm.my

structure is motivated by a concern for protecting the coastal area for wetland rehabilitation, enhancing marine life, and at the same time protecting the shore line. For these reasons, the structure has been designed to be porous enough, unlike the rubble mound breakwaters, such that it allows the flow of water around it and the same time is stable enough to be installed over soft soil. It is proposed that the structure act as an alternative perimeter protection to young mangrove seedlings by enhancing sedimentation build-up in soft muddy coasts due to its ability to dissipate wave energy (Hadibah *et al.*, 2005).

It is realized that there has been no research to develop guidelines for implementing the ArMS system as submerged breakwaters and no previous studies or data are available regarding the transmission, reflection and energy dissipation of wave through ArMS system. Furthermore, no reports have been presented on the optimum configuration and placement of the ArMS system. Therefore with reference to the above considerations, the focus of this paper was to report the numerical results of the hydraulic performance of the ArMS system. Two-dimensional computational model was applied using commercially available Flow-3D® software. The accuracy of the numerical model was verified by comparing the numerical results with the experimental data.

Numerical simulations are carried out to interpret the correlation between the row systems of the ArMS structure which compose of different porosities of 0.75 to 0.95. Each of the porosity was then computed for each structure-row system namely 1-row to 20-row. Various wave conditions were selected to determine the wave transmission as the wave passes over the structure.

2. NUMERICAL MODEL PROCEDURE

Flow-3D® software package is used to examined the hydraulic performance of the ArMS system. The fundamental laws of mass, momentum and energy conservation were adopted in which the finite difference method was applied to solve these equations. The numerical algorithm used was called SOLA-VOF (Solution Algorithm-Volume of Fluid) (Flow Science Inc., 1997). The flow regions are subdivided into a grid of variable-sized rectangular cells. For each cell, values are retained for the basic flow quantities (*e.g.*, velocity, pressure and density). The ArMS geometry in the software was placed in the grids with Fractional Area Volume Obstacle Representation (FAVOR) methods. By doing so, geometry and grid of the structures can be treated independently by this method.

The flow region is subdivided into a mesh of fixed rectangular cells. With each cell there are associated local average values of all dependent variables. All variables are located at the centers of the cells except for velocities, which are located at cell faces (staggered grid arrangement). When free surfaces of fluid interfaces were present, it was necessary to identify whether those cells were empty, contained a partially filled volume, or were full of water. The software considered a cell with an F values less than unity, but with no empty neighbor, as a full cell.

2.1 Global Properties and Criteria

Computational domain with free surface or sharp interface tracking was invoked in this numerical study. Single fluid is implemented throughout the study. Incompressible flow mode is involved in the single fluid. For the single fluid, the volume fraction (F) is occupied by the fluid. Thus, fluid exists where $F=1$, and void regions correspond to locations where $F=0$. "Voids" are regions without fluid mass that have a uniform pressure assigned to them. Physically, they represent regions filled with a vapor or gas whose density is insignificant with respect to the fluid density.

Properties criteria are defined to determine the type of fluid used in the numerical model. In this study, fresh water with density (ρ) = 1.0 gr/cm^3 and kinematic viscosity (ν) = 0.01cm^2/s were selected. Each data were simulated for a total duration of 30s or 40s.

Viscous flow of turbulence with turbulence model was selected in the numerical study. The model consists of two transport equations for the turbulent kinetic energy k and its dissipation ε, the so-called k-ε model. This model has been shown to provide reasonable approximations to many types of flows. Besides turbulence was present in the vicinity of ArMS system, the turbulence model considered is expected to give a better representation of the turbulence around the structures. The wall shear condition was selected in the simulation. Wall shear stresses are modeled by assuming a zero tangential velocity on the portion of any area closed to flow. Gravitational acceleration in z direction of 980 cm/s^2 is considered dominant, since only 2 dimensional flow in the x and z directions were implemented.

2.2 Physical Consideration

As the mangrove roots in the physical model are rather complicated, it is impractical to exactly reproduce the mangrove geometry in the numerical domain. Instead, a simpler and uniformly distributed material having a particle diameter, *D* was assumed as representation of the mangrove trunk and root systems. Fig. 1 shows the definition sketch of the ArMS submerged breakwater used in the physical model tests while Fig.2 illustrates the transformation from physical to numerical geometry. The area bounded by ABCD is considered as representative of the ArMS system whereby the actual porosity is uniformly distributed. The numerical porosity is defined as the ratio of the volume of empty space (V_e) in a physical model (Eldina, 2007) to the total model volume (V_t). In this case the total model volume is defined as the numerical geometric control volume of 21.5 cm x 21.5 cm x 21.5 cm. Hence correlation between experimental porosity and numerical porosity as given in Fig.3 are required to accommodate the transformation of the control unit volume used between the experimental and numerical.

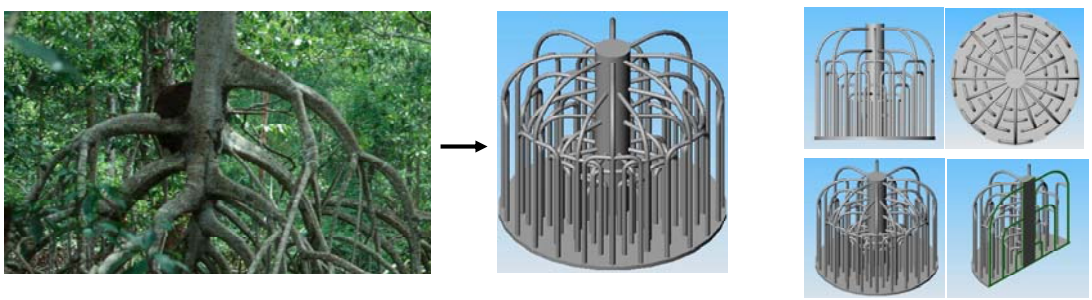

Figure 1 : Experimental geometry of the ArMS system

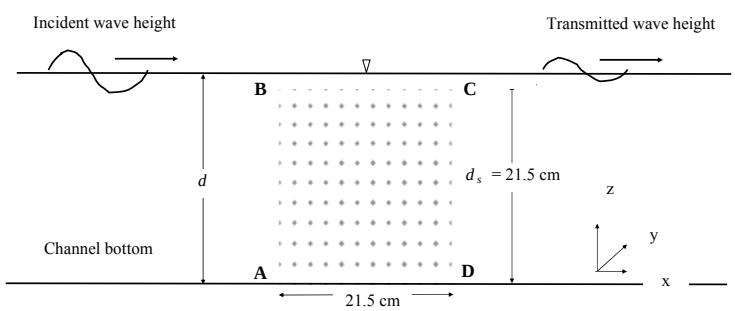

Figure 2 : Side view of the representation of the ArMS system

It can be described here that for the experimental porosity of 0.88 and 0.83 is relevant to the numerical porosity of 0.95 and 0.94 based on Fig. 3.

It must be noted that there is little physical sense in employing a porous media flow model, e.g., using porous obstacle and baffles, without defining flow loss coefficients. Linear and quadratic flow loss equations can be combined into a single expression for the drag coefficient and this dependence is a function of the local Reynolds number based on the average particle diameter *D*:

$$K = \frac{\mu}{\rho}\frac{1-V_F}{V_F^2}\left[ADRG\,(1-V_F) + BDRG\,\frac{R_e}{D}\right] \tag{1}$$

where, μ = viscosity of the fluid,

ρ = the density of the fluid,

ADRG and BDRG = drag parameters used in Flow-3D®,

R_e = $\frac{\rho u D}{\mu}$ = Reynolds Numbers

ADRG = $\frac{\alpha}{D^2}$ and *BDRG* = $\frac{\beta}{D}$, where *D* is the "average particle" (representing the ArMS trunk, main and secondary roots) diameter in the porous structure, α is a constant that typically has a value of 180 and β is a roughness factor which ranges between 1.8 and 4.0 (representing smooth to rough particles) (Flow Science, 1997). In this study a β value of 1.8 was selected and the structure considered has smooth surface. Porosity of the structure (ζ_n) is specified by the volume fraction (V_F) in the computational procedure. The porosity can vary between 0.0 (no porosity – the same as a completely solid obstacle) and 1.0 (fully open region). It should be noted that porosity cannot be time dependent. Based on the consideration of α = 180 and β = 1.8 the range of average particle of *D* can be generated and drag parameters of ADRG and BDRG can be obtained as given in Figs. 4 and 5 respectively. One can see that these parameters decrease exponentially with *D*.

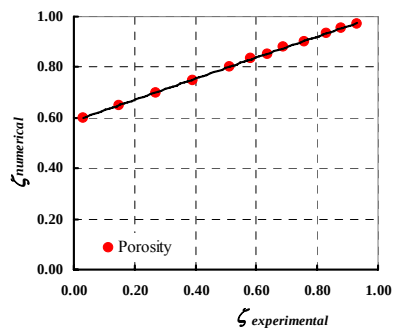

Figure 3 : Correlation between experimental and numerical porosities

Regions containing arrays of many small obstructions as shown in Fig. 1 that are too small to be individually resolved can be modeled by using a distributed volume reduction. In Flow-3D® this is modeled with porous obstacles. The code's obstacle generator can be used to define obstacles having different values of porosity and different ADRG and BDRG coefficients.

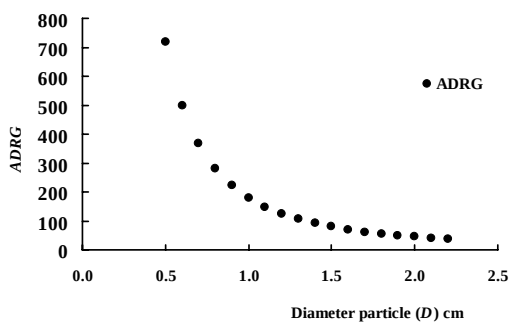

Figure 4 : Relationship between diameter particle *D* with ADRG

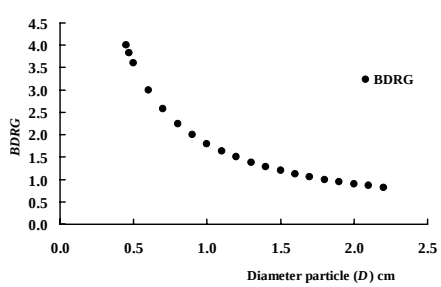

Figure 5 : Relationship between diameter particle *D* with BDRG

In order to gain the physical meaning of the numerical porosity, the set of empirical coefficients, ADRG and BDRG, in the governing equations describing flow in porous structures was determined using a

simple method. The method is to use the ArMS submerged breakwater's transmission coefficients data from experimental work, then to simulate numerically to obtain each value of transmission coefficients by trying various particle diameter (*D*) values. Finally, we select the *D* value, whose corresponding numerical transmission coefficients fit best into the experimental data.

2.3 Meshing and Geometry Interpretation

The associated 'Numerical Wave Tank' is modeled in correspondent with the geometry of the wave flume available in the Hydraulics Laboratory of the Coastal and Offshore Engineering Institute at Universiti Technologi Malaysia. The computational domain in this study was extended, such that the wave does not reach the downstream boundary of the domain, while the height of the tank was also reduced to save the computer memory.

The numerical wave flume is divided into 3 regions with different rectangular-grid densities. It consists of an upstream, the representative geometry, and a downstream region behind the ArMS system respectively. Typical example of the numerical domain is illustrated in Fig. 6. According to Clauss and Habel (2000) good results were achieved by modeling the wave tank 2-3 wave lengths in front of the investigated area and 4-6 wave length behind. In this study, about 2 and half wave length (the longest wave length tested) of 800 cm at the upstream region was used while longer downstream channel length of 4200 cm was used avoid numerical instability.

The mesh cells occupied by the representative geometry (obstacle) will be flagged automatically by Flow-3D®. The portions of element surfaces and volumes blocked by the obstacles were computed and stored before starting the hydrodynamic calculation. The quantity chosen as flag was the volume fraction. When this quantity is zero, the cell was entirely within the obstacles and all fluid calculations in the cell were eliminated. No velocity or pressures were computed in full ArMS obstacle cells, and all velocity components on faces of obstacle cells were set to zero. Therefore the cells were numerically blocked by the obstacles.

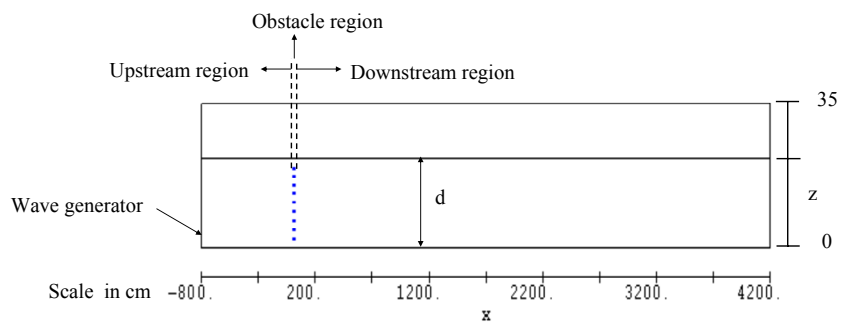

Figure 6 : Typical example of numerical domain with water depth of *d* = 22.0cm, extended from x = – 800.0 cm to + 4200.0 cm and from z = + 0.0 cm to 35.0cm

The obstacle were placed on the wave tank base using a Cartesian two-dimensional coordinate system (*x* and *z*) from the 0.0 cm to a distance depending on the structure arrangement (in terms of the width of the obstacle), in the downstream direction. Structure geometry is then defined within the grid by computing the fractional face areas and fractional volumes of each element that are blocked by the obstacles. Fine meshes of 1.0 cm, horizontally, were generated in the geometry region. Mesh size of 5 cm were imposed at the upstream and downstream of the obstacle respectively.

The grids used to cover the area of computation were 1087 in the horizontal direction. In the upstream areas of – 800.0 cm to the x position of 0.0 cm, the total cells were 160. Number of cells from x = 0.0 cm to x = + 107.5 cm (if the structure width, *W* = 107.5 cm) where the obstacles seated were 108, while in the downstream areas, starting from + 107.5 cm to 4200.0 cm, total number of cell were 819. In the vertical direction, total numbers of cells were 17 over a height of 35 cm (each cell being 2.0 cm in height). Therefore, the total cells used in both directions were 18479. These grids were used to cover the physical size of the computational domain which was 5000.0 cm in length and 35.0 cm in height. This length is sufficient for avoiding fluid accumulation that would induce mass conservation imbalance in the numerical computational process.

The actual number of cells created by the mesh generator may differ from the specified value since the generator attempts to smooth the mesh. It is found that the smallest cell sizes in the x and z directions were 1.0 cm and 1.93 cm respectively. The largest cell size for both x and z directions were 8.99 cm and 2.33 cm respectively. Maximum adjacent cell size ratios were 1.05 and 1.020 for both x and z directions. This cell ratio is obtained by dividing between adjacent cells. For accurate and efficient results, the size ratio between adjacent cells should be as close to unity as possible, and not exceed 1.25 (Flow Science, 1997).

2.4 Boundaries Determination

At the mesh boundaries, a variety of conditions could be set using the layer of fictitious cells surrounding the mesh. Six types of boundary conditions were provided by Flow-3D®; symmetry plane (default), specific velocity, continuative, rigid wall, specified pressure, and periodic boundary condition. However in this study only the first three were adopted.

Generally, all rigid and free boundary surfaces are treated as free-slip boundaries (no tangential stresses on the surfaces) and referred to as symmetry plane boundary condition. For rigid wall boundary, the normal and tangential velocities are set to zero. However, in the no-slip wall conditions, the tangential velocity can be set to any value by the wall shear stress model provided by the software. In the specified velocity condition, tangential velocities and normal velocities must be specified. These boundary conditions are specified for the right, top and bottom boundaries of the mesh.

The wave tank top and bottom are defined as symmetry boundaries. For wave propagation problems, special boundary treatments have been devised in Flow-3D® (Flow Science, 1997). The outflow boundary condition or right boundary is set in term of continuation condition such that a minimum reflection allowed. Fig. 7 illustrates the application of the boundary conditions in the numerical model.

A wave maker located at the left boundary generates waves propagating from left to right. The wave maker imposed fluid velocity according to the linear wave theory. A special boundary condition for a linear, periodic wave in the x direction is specified at the left boundary. Dummy variables have been used to set the wave properties namely wave frequency ($\frac{2\pi}{T}$), wave number ($\frac{2\pi}{L}$) and incident wave height (H_i). The waves are gravity driven. Initial values for the simulation start (t=0) should be declared first by providing the SWL water depth at the left boundary.

The locations of numerical wave probes were similar to those in the experiment flume. Five probes were installed in the upstream zone while 2 others were installed at the downstream region. Probe 1 which was used to input incident wave heights (H_i) was set at – 500.0 cm (with the assumption that no reflection effect from the obstacle) and probe 2, 3, 4, and 5 were put at -135.0 cm, -105.0cm, - 75.0 cm, and -60.0 cm respectively. In the downstream region, probes 6 and 7 were located at + 100.0cm and +269.0cm fro all conditions, except for the 20-row system, where probe 6 and 7 are located at + 400 cm and + 500 cm respectively.

2.5 Initial Conditions

Initial field of hydrostatic pressure in z direction was specified in the model. Water depths of 20.0 was applied and water surface is considered to be at rest. Pressure iteration of line implicit in *x* and *z* direction and first order momentum advection were adopted in this study. “Solve all fluid transport equations” was selected in the fluid flow solver selection options (Flow Science, 1997). The numerical calculations were carried out using in a Pentium (R) D CPU 3.00GHz with 3.24 GB of RAM. CPU time required to simulate a typical problem was about 15 to 25.0 minutes.

3. Numerical Model Test Cases

Extensive numerical investigations were conducted to examine the performance of different representative geometries of ArMS system. Experimental data used for numerical model validation were taken based on data collected from Eldina (2007). Incident wave heights (H_i) used as input data which were taken from the experimental data after the reflection wave heights have been separated.

Table 1 exhibits the scenario of the numerical simulation test cases. In case of AA numerical test, one can see that, there are 40 calculations should be carried out with the condition of water depth = 22.0 cm, 7 different values of porosities, 5 different row arrangements (different structure width), and at 2

initial wave conditions. It should be noted that for simplification and in order to get the relative structure heights variations, the structure heights were varied instead of the water depth. Thus water depth of 22.0 cm was kept constant for all the numerical test cases conducted. There were about 210 test cases investigated in this numerical study.

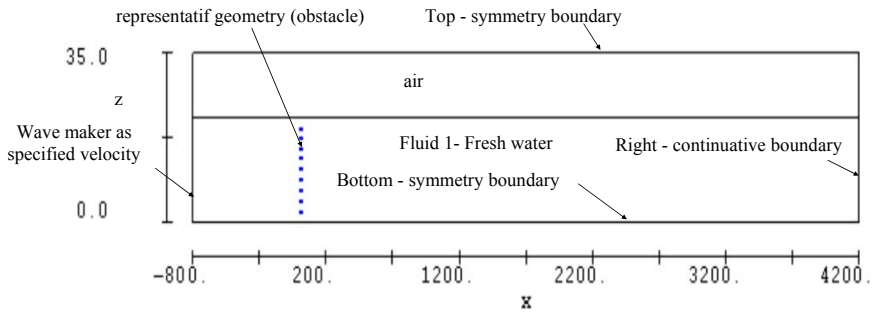

Figure 7 : Numerical boundary conditions adopted in this study

Case	d (cm)	d_s (cm)	G_s (cm)	ζ_n	Rows n	Rows W (cm)	H_i (cm)	T (s)
AA	22.00	21.50	0.00	0.75 0.80 0.83 0.85 0.88 0.90 0.95	1 3 5 9 20	21.50 64.50 107.50 193.50 430.00	1.50 5.50	2.00 1.40
		1		7	5		2	
BB		21.5		0.85 0.90 0.95	1 3 5 9 20	21.50 64.50 107.50 193.50 430.00	5.50	0.75
		1		3	5		1	
CC		21.50		0.95	1 3 5 9 20	21.50 64.50 107.50 193.50 430.00	1.50 2.50 4.50 5.50 6.20 6.10 5.50 5.50	2.00 1.80 1.60 1.40 1.20 1.00 0.80 0.75
		1		1	5		8	
DD		28.00 18.00 14.00 10.00		0.75 0.80 0.83 0.85 0.88 0.90	5		1.5	2.0
		4		6	1		2	
EE		28.00 18.00 14.00 10.00		0.95	1 3 5 9 20	21.50 64.50 107.50 193.50 430.00	1.50 5.50	2.00 1.40
		4		1	5		2	
FF		21.50		0.95&0.94 0.95&0.94&0.75	5		1.50 2.50 4.50 5.50 6.20 6.10 5.50 5.50	2.00 1.80 1.60 1.40 1.20 1.00 0.80 0.75
				2	1		8	
			5.00 10.00 15.00 20.00 25.00 30.00 100.00	0.95&0.94 0.83	5		1.50	2.00
	1	1	7	2	1		1	

Table 1 : Numerical simulation test cases

4. Verification of the Numerical Model

The accuracy of the numerical computation domain investigated as well as the suitability of the parameters selected were first verified before conducting any further study on the waves and the ArMS structures. The first step was to simulate the wave profile without the structure, and then to compare the wave profiles with those experimented with the same wave conditions. Fig. 8 shows an example of comparison between experimental and numerical water surface fluctuation without the structure at selected probes with wave conditions of H_{ie} = 4.2 cm and T_{in} = 1.23s, and at water depth of 22.0 cm. It is found that the qualitative behavior of the computed results was captured reasonably well, although few discrepancies were observed between measured and computed values.

Verification between numerical and experimental results is interpreted in terms of wave transmission coefficient, since this dimensionless parameter is normally used to define wave-structure relationship in coastal engineering design. Wave transmission coefficient in numerical results (C_{tn}) were defined as the ratio of incident wave height (H_{in}) at x = -500.0 cm with the transmitted wave height (H_{tn}) recorded at x = + 269.0 cm.

In the numerical simulation, trial and error justifications were carried out to determine the best fit of drag parameter of ADRG and BDRG. First step was to simulate the wave flow passing over the structure where the influence of volume fraction and Reynolds number (R_e) were taken into account for all test cases. The results of these best fit investigations are typically shown in Figs. 9 and 10. Fig. 9 shows the relationship between the predicted and measured wave transmission coefficients and incident wave heights with D = 2.0 cm and calculated values of ADRG = 45 and BDRG = 0.9 while Fig.10 with D = 0.6 cm and calculated value of ADRG = 500 and BDRG = 3.0. These cases were simulated for water depths of 22.0 cm, 5-row system, and porosity of 0.95 & 0.94. In the second a straight line was plotted for the case where the experimental and theoretical results are the same.

From Fig. 9 one can see that the values of numerical transmission coefficients with respect to experimental transmission coefficients are found overestimated. The prediction of D = 2.0 cm is not properly fitted to the straight line. The data points are beyond the range of ± 10% of the line based. However when the value of D was reduced to 0.6 cm, the comparison between the C_{tn} and C_t are relatively good throughout the range of data calculated. All of the data points fall within the ± 10% as given in Fig.10.

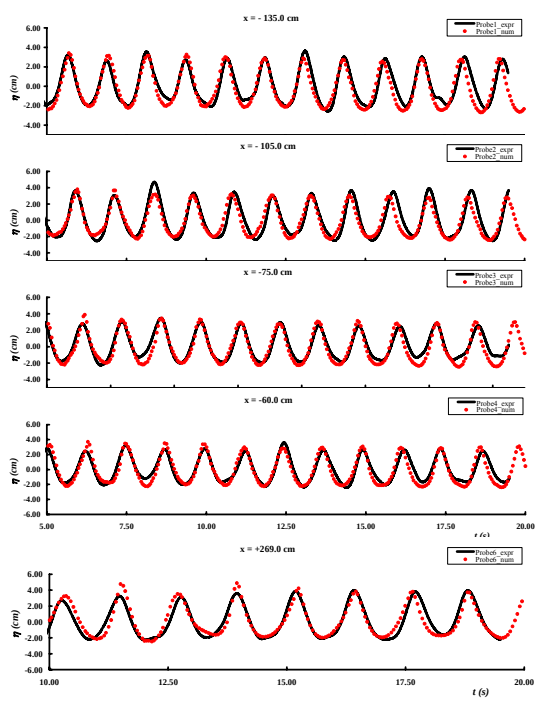

Figure 8 : Wave profiles recorded at several stations for incident waves height (H_i) = 4.20 cm, T = 1.23s, and d = 22.0 cm (without the structure)

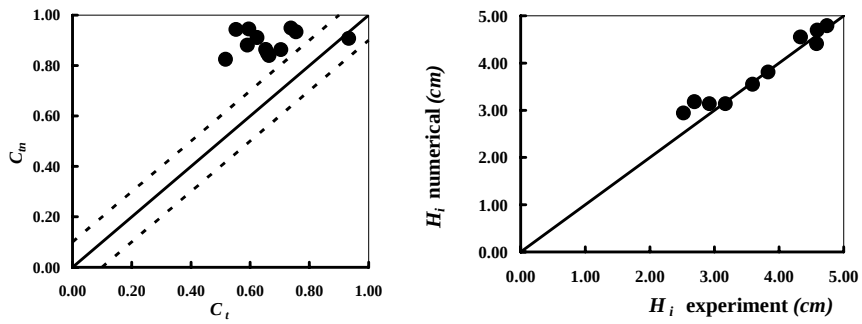

Figure 9 : Numerical and experimental wave transmission coefficients with *D* = 2.0 cm

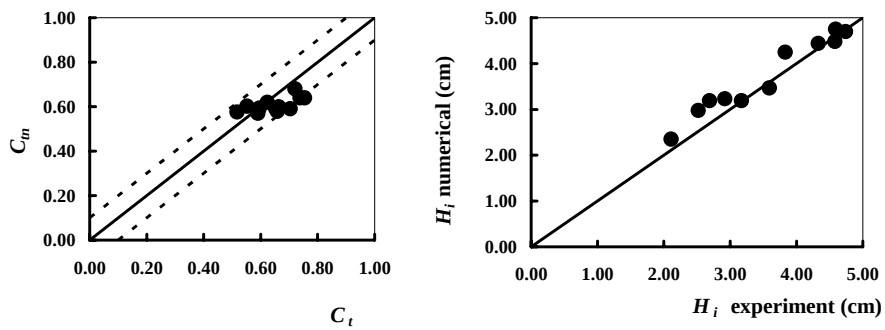

Figure 10 : Numerical and experimental wave transmission coefficients with *D* = 0.6 cm

5. NUMERICAL RESULTS AND DISCUSSION

Test cases that have been computed numerically are discussed in terms of dimensionless parameters. The influence of porosity, relative structure heights, wave steepness, relative structure width in terms of the row system, and also the porosity variations within a specified row system on the wave transmission coefficients are investigated in this section.

5.1 Analysis of Numerical Results

5.1.1 Effect of Porosity (ζ_n) and Number of Rows vs Wave Transmission Coefficient (C_{tn})

The effects of porosity of the structure on the wave transmission coefficient with 1- to 20-row systems are studied. Structures with different porosities of 0.75 to 0.95 are computed at a relative water depth of 1.0 and wave steepness of 0.005 and 0.03. Their relationships with the wave transmission coefficients are shown in Figs. 11 to 13 respectively. Fig. 1 shows that the wave transmission coefficients decrease as the porosities decrease. 1-row system can only reduce wave energy up to 0.83 while 20-row system can reduce wave height as low as 0.01 when the porosity is 0.75. If wave transmission coefficients were to be designed as high as 0.5, the ArMS structure should be constructed in a 20-row system with a porosity of 0.95. However if the porosity is reduced to 0.8 the structure row number is reduced to 5 to get the same wave transmission coefficient of 0.5. It saves the construction cost significantly.

Similar characteristics can be found in Fig. 12. However in this plot for a 1-row system with porosity of 0.75 the wave transmission coefficient is found to be 0.66 and similarly a 20-row system would produce a wave transmission coefficient of almost 0.0. In this condition the wave energy is completely dissipated inside the structure and the region in the leeside is very calm.

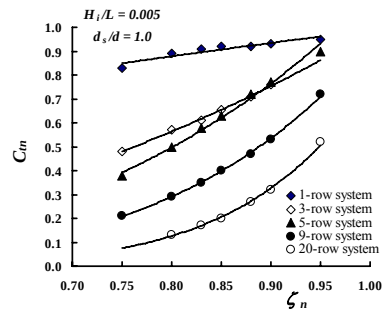

Figure 11 : Effect of porosity and number of rows vs wave transmission coefficient (C_{tn}) (d_s/d = 1.0 and H_i/L = 0.005)

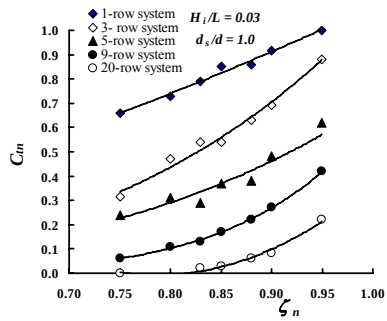

Figure 12 : Effect of porosity and number of rows vs wave transmission coefficient (C_{tn}) (d_s/d = 1.0 and H_i/L = 0.03)

Clear influence of porosity and wave steepness on wave transmission is illustrated in Fig. 3. Keeping the structure row system to 5, it is observed that low relative wave height exhibits high wave transmission coefficients for all porosities investigated conversely high relative wave height results in low wave transmission coefficient. Further investigation on the effect of wave steepness on the number of rows in the system will be elaborated in the next part.

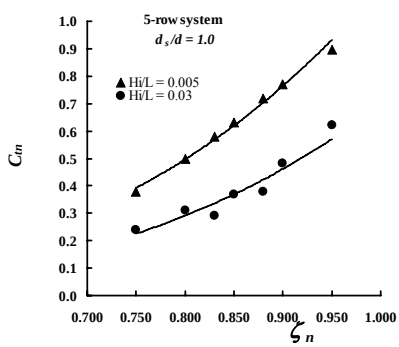

Figure 13 : Effect of porosity and wave steepness (H_i/L) vs wave transmission coefficient (C_{tn}) (5-row system and d_s/d = 1.0)

5.1.2 Effect of Wave Steepness (H_i/L) and Number of Rows vs Wave Transmission Coefficients (C_{tn})

Investigating wave steepness (H_i/L) is necessary to understand the performance of the structure. The effect of wave steepness on C_{tn} for different row numbers (1- to 20-row systems) for specified porosity of 0.95 is provided in Fig. 14. It is found that the wave transmission coefficient decreases sharply as wave steepness increases in the region of 0.005 to 0.04 for all the structure systems considered. However, when the relative wave steepness is greater than 0.04 the wave transmission coefficients tend to be constant. The same decreasing trends among the row systems considered can also be

observed. As expected the higher the number of rows, the higher the energy that can be absorbed. This fact can be explained as follow. The energy produced by wave with low wave steepness (wave with short wave period) can be easily absorbed when the wave propagates over the porous structure. On the other hand wave with high wave steepness (wave with long wave period) does not have enough time to "feel" the structure effect as it passes over the structure. Thus most of its energy is transmitted to the shore.

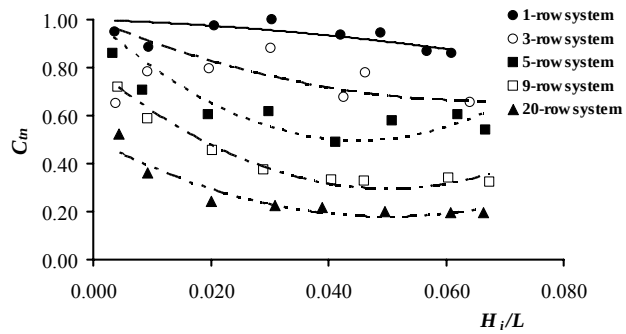

Figure 14 : Effect of wave steepness (H_i/L) and number of rows vs wave transmission coefficient (C_{tn}) (ζ_n = 0.95 and d_s/d = 1.0)

5.1.3 Effect of Relative Structure Width (W/L) vs Wave Transmission Coefficients (C_{tn})

In this study we also determine the width of the structure in terms of row number because ArMS structure is designed as a unit (one unit has diameter of 21.5 cm). Hence when we mention *W* as a width parameter it is also meant as row system as a whole.

When the relative structure widths are extended to 5.5 (for 20-row system) the wave transmission coefficients could be dropped to 0.2 as shown in Fig. 15. It seems that almost all of wave energy is dissipated within the structure and only a small portion of it is transformed to the shore. It is very obvious that the longer the structure the greater the wave that could be absorbed. The decreasing curve explains exactly the effect of the structure width on the wave transmission coefficients.

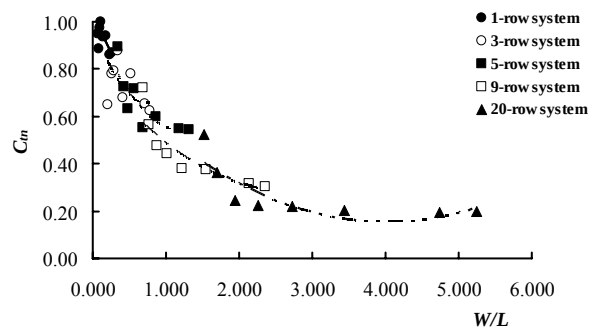

Figure 15 : Effect of relative structure width (*W/L*) and number of rows vs wave transmission coefficient (C_{tn}) (ζ_n = 0.95 and d_s/d = 1.0)

For the *W* = 1.0 to 20 of wave length *L*, the wave transmission coefficient is found to be 0.44 and 0.55 for 9- and 5-row system respectively at a porosity of 0.95 and d_s/d = 1.0. While C_{tn} for 1- to 3-row system are only found above 0.62. One- to 3-row systems is not be able to protect the shore line when the *W/L* is greater than 0.8.

The next set of figures show the variation of porosity and *W/L* with respect to wave transmission coefficient. In the condition of wave steepness = 0.005 as seen in Fig. 16, one can observe that higher porosity results in higher wave transmission coefficient. At the same time extending the relative structure width will reduce wave transmission for all porosities considered.

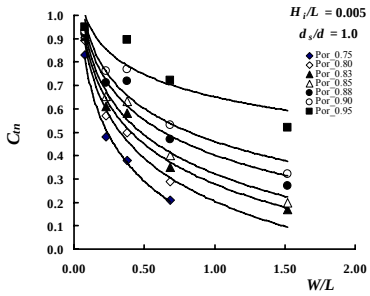

Figure 16 : Effect of relative structure width (*W/L*) and porosity (ζ_n) vs wave transmission coefficient (C_{tn}) (d_s/d = 1.0 and H_i/L = 0.005)

The ability of the submerged breakwater to withstand wave action having water depth equal to the structure height is strongly influenced by its porosity as well as its width. The smaller the porosity the higher is the wave energy absorption. More over the wider the structure the smaller the wave transmission coefficient is. Structures with porosities of 0.95 to 0.75 transmit almost all of the wave energy they receive (wave transmission coefficients $\geq$ 0.8) when *W/L* = 0.08. But the wave transmission coefficients can be dropped to below 0.52 provided the relative structure width is extended to 0.5 as illustrated in Fig. 16.

For the case of wave steepness $\geq$ 0.03 as plotted in Figs. 17 and 18, structure with a width of greater than one wave length can reach a wave transmission coefficient as high as 0.55 for all porosities considered. If one wants to design the ArMS structure which can absorb the wave energy less than 50% and in the extreme wave condition, then one should select the structure with a relative structure width $\geq$ 0.68.

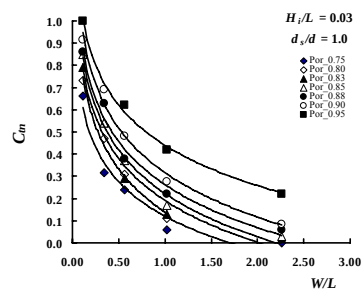

Figure 17 : Effect of relative structure width (*W/L*) and porosity (ζ_n) vs wave transmission coefficient (C_{tn}) (d_s/d = 1.0 and H_i/L = 0.03)

The next effort is to determine the porosity. Porosity of 0.75 technically is the best choice since the structure with this porosity can absorb wave energy up to 21% but it is very costly. Selecting porosity of 0.8 or 0.85 is suggested for the sake of efficiency. We should bear in mind that ArMS structure is designed as a very porous geometry, hence with porosity of 0.8 or 0.85 the structure is still able to absorb wave energy up to 50% provided the structure is designed with a minimum relative structure width of 0.68. More over, having very porous structure is really intended for the case of protecting the wetland habitat restoration. Beside provides good water circulation offshore it does not disturb the sea creature pathway.

Twu and Chieu (2000) has pointed out that a single layer offshore breakwater was shown to reduce the coefficients of transmission and reflection only when the structure is very wide and the material have a high porosity. However, a multilayer breakwater can function well in reducing wave transmission coefficient at a lesser width. We conducted a series of numerical tests with 5-row system having porosity of 0.95&0.85&0.75 (2 rows for porosities of 0.95 and 0.85 respectively and one row for porosity of 0.75). Higher porosities are situated facing the incident wave. Results are compared to that of 5-row system having constant porosity of 0.95 only and a combination of 0.95&0.94 respectively as plotted in Fig. 19. It is confirmed from the numerical tests that 5-row system with three different porosities may reduce wave energy better compared to that of 5-row system with one or two number

of porosities for *d/L* less than 0.12. However for *d/L* > 0.15 the effect of varying porosities is not so significant and the wave transmission coefficient tends to stay at the value of 0.4 for porosity of 0.95&0.85&0.75. Facing this fact therefore proper selection of the variation of the porosity should be planned carefully.

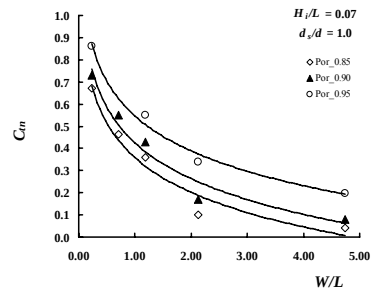

Figure 18 : Effect of relative structure width (*W/L*) and porosity (ζ_n) vs wave transmission coefficient (C_{tn}) (d_s/d = 1.0 and H_i/L = 0.07)

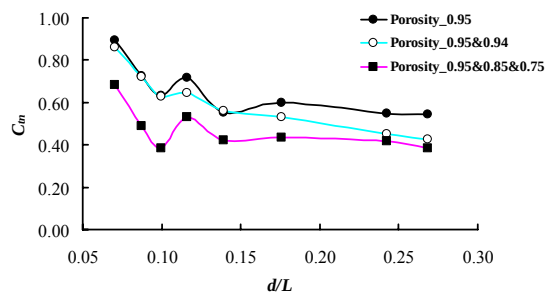

Figure 19 : Effect of relative water depth (*d/L*) and multi layer systems vs wave transmission coefficient (C_{tn}) (d_s/d = 1.0 and 5-row system)

Fig. 20 also informs us that multilayer systems (varying porosity) reduce the width of the structure significantly. Here ratio of structure width to water depth instead of wave length (*L*) was given. It can be figured out that in the case of a 9-row system with porosity of 0.95 wave transmission coefficients reduce to as low as 0.31 whereas a 5-row system with porosity of 0.95&0.85&0.75 may reach wave transmission coefficient reduction up to 0.34. Thus in this case considering an ArMS structure with the 5-row system is much more efficient, since the 5-row system is shorter than 9-row system and it still able to give wave transmission coefficients as low as 0.34.

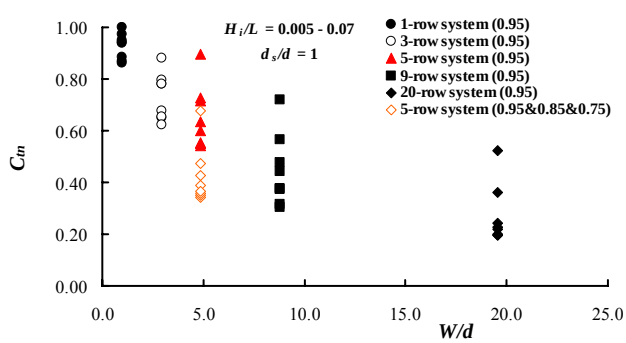

Figure 20 : Effect of structure width (*W/d*) vs wave transmission coefficient (C_{tn}) (ζ_n= 0.95 and 0.95&0.85&0.75, H_i/L = 0.005 – 0.07 and d_s/d = 1.0)

One can reduce the porosity as low as possible (to be impermeable) but this is not recommended since a structure with very low permeability will naturally be reflected the waves. Whereas in order to protect the mangrove restoration site it requires a structure which is porous enough but still be able to

withstand from wave attack during high season. This also explains why a multi layer system should be introduced instead of a single layer to cater for the structure width reduction.

5.1.4 Effect of Relative Water Depth (d/L) and Number of Rows vs Wave Transmission Coefficients (C_{tn})

It is also interesting to investigate the influence of the number of rows in terms of relative water depth. Relative depth is one important parameter in understanding the hydrodynamic characteristics of the submerged structure for coastal and deep water region. Fig. 21 depicts this condition clearly. As *d/L* increases C_{tn} decreases noticeably but when $d/L > 0.15$ it seems C_{tn} remains constant. Let consider the 5-row system only. It can be seen that at the small relative water depth the ability of the structure to absorb the wave energy is weak compared to the high relative water depth. This means that a long wave may transmit a considerable percentage of wave energy into the structure's lee side. Thus there is less chance for the wave energy to be dissipated over the porous submerged structure. To improve this situation, we now consider the structure with a 9-row system. It is found that the transmission coefficient is reduced considerably when compared to the structure with a 5-row system. It is therefore concluded that ArMS submerged breakwater can meet the demand of low values in wave transmission coefficients provided the structure is of considerable thickness (in terms of row system) and the geometry has a high porosity (here the porosity is 0.95).

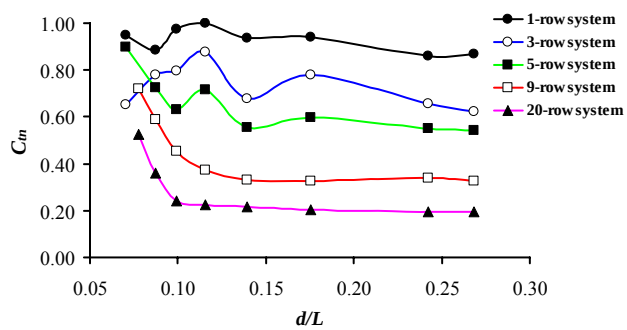

Figure 21 : Effect of relative water depth (*d/L*) and number of rows vs wave transmission coefficient (C_{tn}) (ζ_n = 0.95 and d_s/d = 1.0)

5.1.5 Effect of Relative Wave Height (H_{in}/d) and Number of Rows vs Wave Transmission Coefficients (C_{tn})

Fig. 22 illustrates the influence of relative wave height and structures row system on C_{tn} for d_s/d =1 and constant porosity of 0.95. It is found that increasing the relative wave height will decrease the wave transmission coefficients for different row numbers. It seems that at H_i/d greater than 0.2, the wave transmission coefficient tends to be constant; it does not vary significantly for all structure conditions. This can be seen clearly for the 9- and 20-row system structures.

Submerged breakwaters have proven to be effective wave control structures, and are extensively used for coastal protection. Submergence below the water surface and the porosity of the breakwater allow part of the incident wave energy to pass through the structure, and only a small part to reflect from the structure. Although the structure allows some wave energy transmission into the protected zone, the turbulence generated in the porous medium dissipates it sufficiently. Depending upon the tranquility requirements of water, area intended for protection, and prevailing littoral movement condition, the porous breakwater can be designed suitably (Hutchinson and Raudkivi, 1984).

One method of increasing the turbulence is by providing more perforations on the surface of the structures such as in our ArMS structure by reducing the root diameter and adding more main or secondary root numbers. Irregularity and a rough surface texture of the structure, as well as the vertical structure profile will affect sea living creature enhancement.

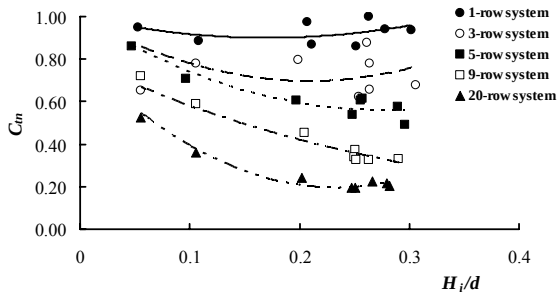

Figure 22 : Effect of relative wave height (H_i/d) and number of rows vs wave transmission coefficient (C_{tn}) (ζ_n = 0.95 and d_s/d = 1.0)

5.1.6 *Effect of Relative Structure Height (d_s/d) and Number of Rows vs Wave Transmission Coefficients (C_{tn})*

The non dimensional parameter of relative structure height is important to understand the selection of an appropriate structure configuration as required from the hydrodynamic performance and aesthetic consideration. The effect of relative structure height on C_{tn}, for H_i/L =0.005 and 0.03, porosity of 0.9 is shown in Figs. 23 and 24.

It is interesting to note from Fig. 23 that for row number of 1, 3 and 5, C_{tn} slightly decreases as d_s/d increases. The value of C_{tn} remains above 0.8 for these conditions. This is due to the fact that 1-, 3- and 5-row system with porosity of 0.95 is less effective to absorb the wave energy for low wave steepness. There is no chance of the structure to dissipate the energy once the wave travels over it (free passage of wave energy). However in the cases of 9- and 20-row system, increases in d_s/d results in a considerable reduction in the C_{tn} value. Optimum C_{tn} value is found as d_s/d = 1.55 since at this condition the top of the structure is above still water and wave propagation can be dissipated better.

In fact, having the structure emerging to the surface is not good aesthetically even though it may reach optimum wave absorption, it is not recommended to install the structure at this conditions. Therefore selecting proper structure height and water depth ratio is also important.

Fig. 24 shows relatively similar characteristics to those found in Fig. 23. But here all row number systems have greater ability to absorb wave energy as expected. It is found that as d_s/d increases C_{tn} value decreases prominently. At relative structure height of 1.0, a 5-row system can reach C_{tn} equals to 0.62, while for 9-row system, the C_{tn} value is found = 0.43. However as d_s/d is less then 0.8 the structures have low capability in absorbing wave energy.

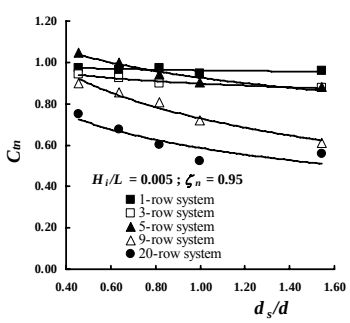

Figure 23 : Effect of relative structure height (d_s/d) and number of rows vs wave transmission coefficient (C_{tn}) (ζ_n = 0.95 and H_i/L = 0.005)

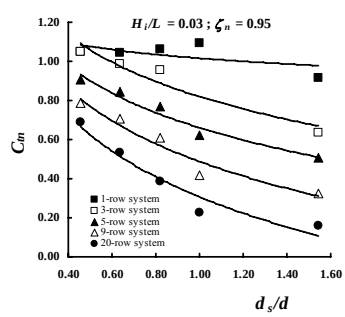

Figure 24 : Effect of relative structure height (d_s/d) and number of rows vs wave transmission coefficient (C_{tn}) (ζ_n = 0.95 and (H_i/L = 0.03)

Fig. 25 shows the effect of relative depth of immersion on C_{tn} for a 5-row system. This plot is provided for H_i/L = 0.005 and 0.03. It is to be noted that a negative value of Δ/d indicates the structure is submerged, while a positive value is when the structure is above the still water level. For Δ/d=0.0 it indicates that the top of the vertical structure is at SWL.

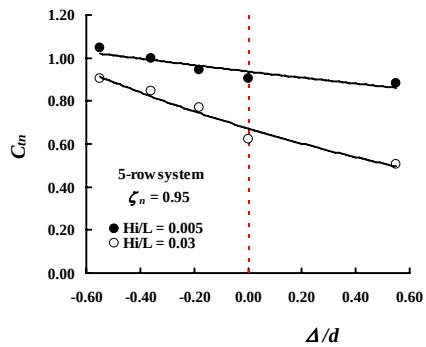

Figure 25 : Effect of relative free boards (Δ/d) vs wave transmission coefficient (C_{tn}) (5-row system, ζ_n = 0.95 and H_i/L = 0.005 and-0.03)

It is found that the transmission is minimized when the vertical structure of the ArMS breakwater emerges above SWL. The reason for the behavior is as follows. In general, the wave energy is more concentrated near SWL. When the vertical barrier of the ArMS breakwater is projecting above SWL, it gives an effective blockage (better wave dissipation effect, due to turbulence and friction effect) of wave propagation. If the same ArMS breakwater is submerged, it provides free passage of the wave energy (poor wave dissipation effect) over its vertical projection. This is the main reason for significant reduction of the C_{tn} value when Δ/d is increased from -0.55 to +0.55. Hence, it can be concluded that the ArMS break water in the emerged condition is efficient in reducing the wave transmission. This shows that the ArMS breakwater is also a good wave energy dissipater.

Fig. 26 illustrates the influence of porosities with respect to wave transmission coefficients at various relative structure heights. One can see that, the porosities have significant effect on the structure performance in absorbing the wave energy. It is noteworthy to mention that structure with high porosity will absorb less wave energy than that of structure with low porosity at the typical relative structure height.

5.1.7 Effect of Porosities (ζ_n) and Number of Rows vs Wave Reflection Coefficients (C_{rn}) and Energy Dissipation Coefficients (C_{ln})

Twu and Chieu (2000) have investigated numerically the effect of porosity on the reflection coefficient for a single-layer porous structure with porosity of 0.2, 0.5 and 0.8. They concluded that the wave reflection coefficient increases with decreasing porosity. In our numerical calculation we also found that the reflection coefficients decrease as porosities increase as plotted in Fig. 27. It is interesting to note that wave reflection coefficients do not show clear variation for 1- to 9-row system when the porosity is the same. This phenomenon can be seen clearly in Fig. 28.

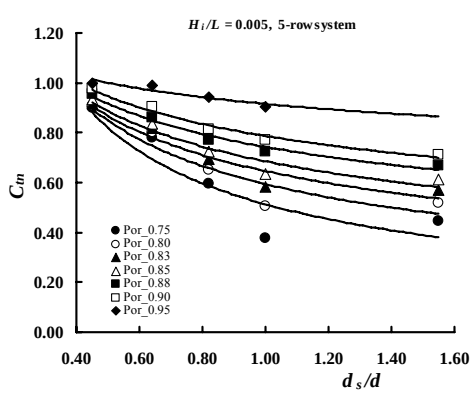

Fig. 26 : Effect of relative structure height (d_s/d) and porosities (ζ_n) vs wave transmission coefficient (C_{tn}) (5-row system and H_i/L = 0.005)

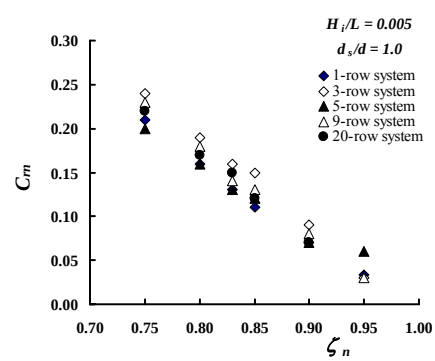

Figure 27 : Effect of porosity (ζ_n) and number of rows vs wave reflection coefficient (C_{rn}) (d_s/d = 1.0 and H_i/L = 0.005)

Under various wave conditions wave reflection coefficients of 5-, 9- and 20-row system do not vary noticeably. The values retain below 20%. It is noteworthy to conclude that the ArMS structure does not reflect the incoming incident wave but dissipate the wave energy instead. Hence it does not produce a significant return force. For that we can mention that the structure does not face any scouring problem in front of the structure toe and the structure can be more stable from overturning. But we have to consider the possibility of structure lifting. Further study on the structure stability should be conducted to solve this problem.

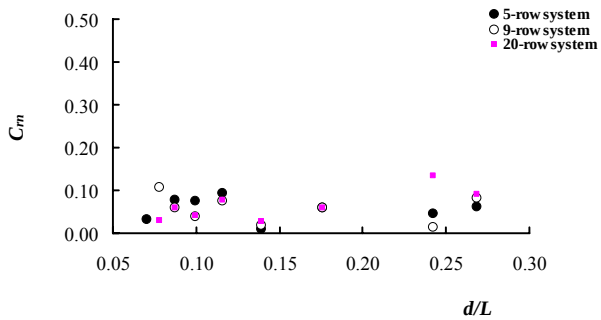

Figure 28 : Effect of relative water depth (*d/L*) and number of rows vs wave reflection coefficient (C_{rn}) (ζ_n = 0.95 and d_s/d = 1.0)

Fig. 29 describes the reduction of wave energy with respect to the porosity. Obviously structure with high porosity will have low wave energy dissipation coefficient for all of row numbers considered. For example a 5-row system structure with a porosity of 0.85 can absorb the wave energy almost 78%. About 12% of its energy will be reflected (can be seen from Figure 6.16) and the rest of it is transmitted.

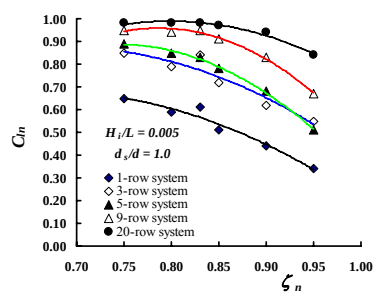

Figure 29 : Effect of porosity (ζ_n) and number of rows vs wave energy dissipation coefficient (C_{ln}) (d_s/d = 1.0 and H_i/L = 0.005)

Fig. 30 illustrates the effect of wave condition with respect to wave energy dissipation coefficient. Wave energy dissipation coefficients tend to increase sharply from the relative water depth (*d/L*) of 0.005 to 0.15 and remain constant when *d/L* greater than 0.5 for all row numbers considered.

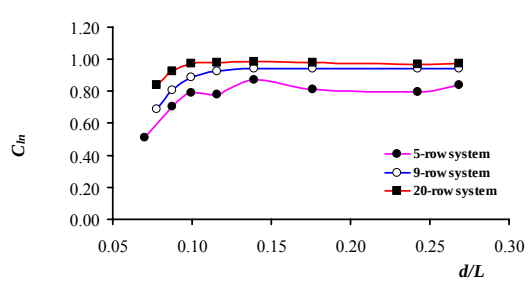

Figure 30 : Effect of relative water depth (*d/L*) and number of rows vs wave energy dissipation coefficient (C_{ln}) (ζ_n = 0.95 and d_s/d = 1.0)

5.2 Comparison between Experimental and Numerical Results

This section will discuss the results obtained from the test cases conducted both through experimental and numerical works. In the computation various drag parameters, ADRG and BDRG, have been tested simultaneously to get the best values. These parameters were then used as the ArMS structure drag parameters thorough the numerical study and comparison of both experiment and numerical results were made. It can be seen from Fig. 31 that computational and experimental data for different relative structure heights agree closely. There is a clear tendency for increasing wave steepness as the wave transmission coefficient decreases. The comparison results also show that reducing the relative structure heights will reduce the ability of the structure to absorb wave energy.

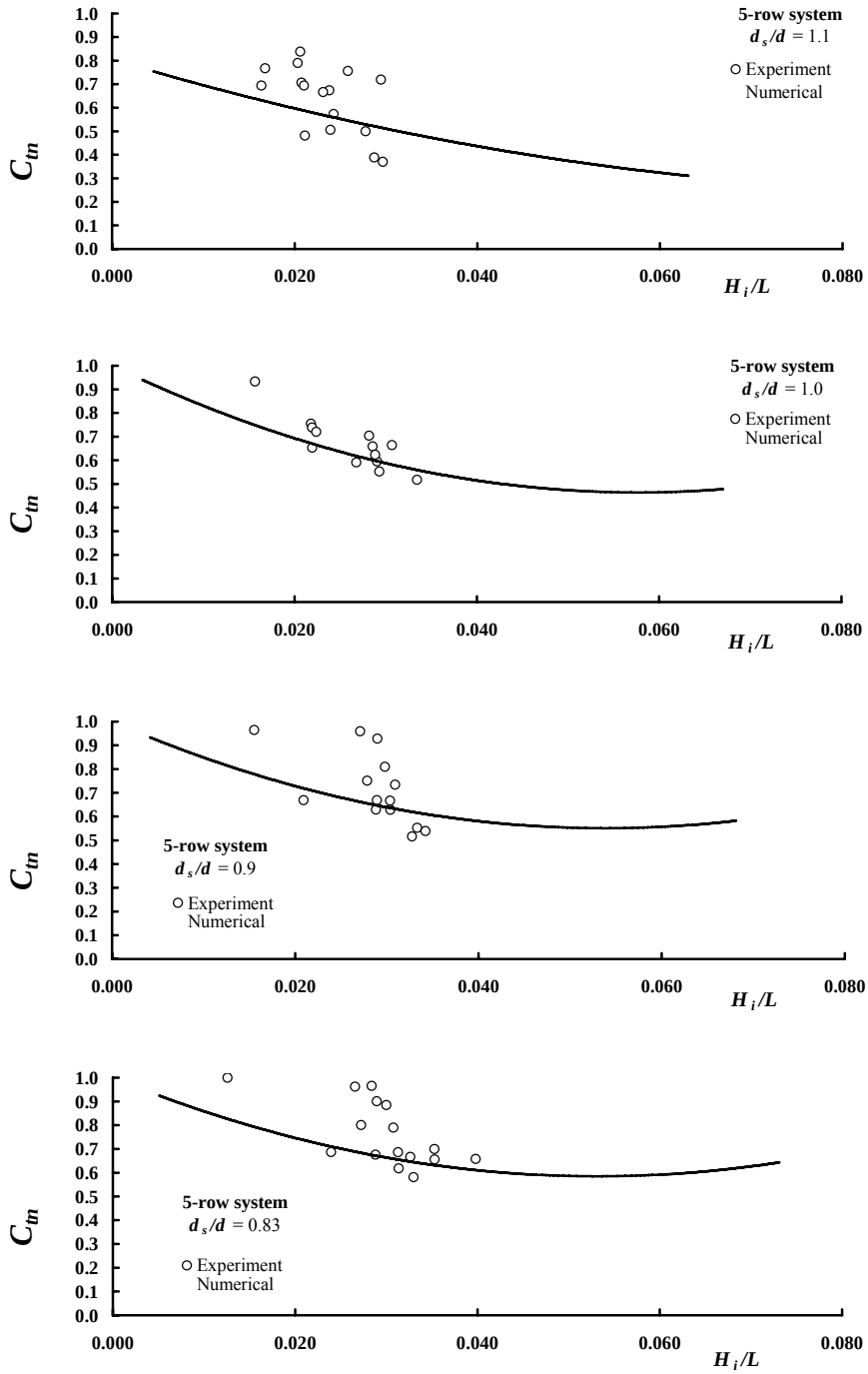

Figure 31 : Comparison between computational and experimental data with respect to wave transmission coefficient (C_{tn}) and wave steepness (H_i/L) (5-row system and various d_s/d)

Fig. 32 shows the typical comparison between numerical and experimental data for the case of 3-row system with the numerical porosity (ζ_n) of 0.95. In this figure, relative wave height is compared with the wave transmission coefficients, it can be seen that the numerical computation can predict well the wave transmission coefficient for the case of 3-row system under various wave condition. It also reveals that C_t decreases as H_i/L increase. It can be seen that the wave transmission coefficients from the experimental study are closed enough to the wave transmission coefficients from the numerical calculation for different wave steepness considered.

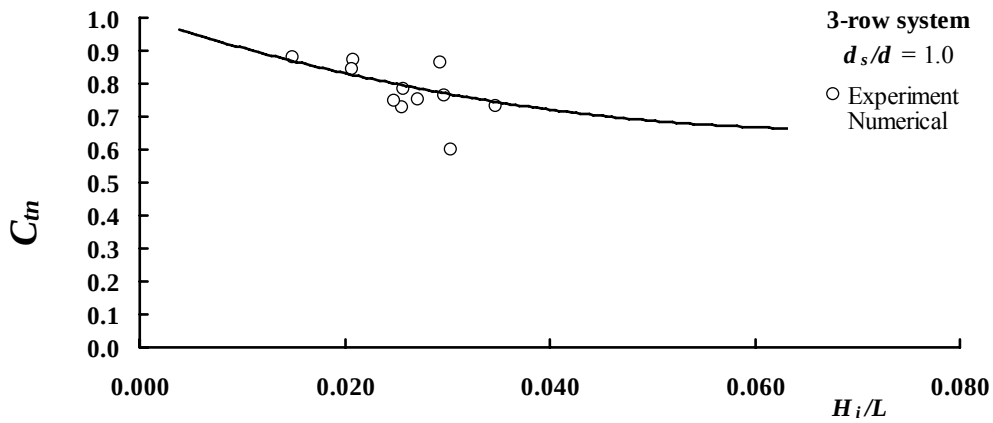

Figure 32 : Comparison between computational and experimental data with respect to wave transmission coefficient (C_{tn}) and wave steepness (H_i/L) (3-row system, ζ_n = 0.95 and d_s/d = 1.0)

6. CONCLUSIONS

Extensive investigation on the numerical and experimental studies has been reported in this paper. The comparison between numerical and experimental data confirms the accuracy of the numerical model.

The numerical results support the following conclusions.

1. The numerical analysis shows that the wave transmission coefficients (C_{tn}) decrease as the porosity (ζ_n) decreases. It was observed that low wave steepness (H_i/L) exhibits high wave transmission coefficients (C_{tn}) for all porosities (ζ_n) investigated conversely high wave steepness (H_i/L) results in low wave transmission coefficient (C_{tn}).

2. The energy produced by wave with low wave steepness (H_i/L) (wave with short wave period) can be easily absorbed when the wave propagate over the porous structure. On the other hand wave with high wave steepness (H_i/L) (wave with long wave period) does not have enough time to “feel” the structure effect as it passes over the structure. Thus most of its energy is transmitted to the shore.

3. The ability of the submerged breakwater to withstand wave action having water depth (d) equal to the structure height (d_s) is strongly influenced by its porosity (ζ_n) as well as its width (W). The smaller the porosity the higher is the wave energy absorption.

4. Relative water depth (d/L) is one important parameter in understanding the hydrodynamic characteristics of the submerged structure for coastal and deep water regions. As relative water depth (d/L) increases the wave transmission coefficient (C_{tn}) decreases noticeably but when d/L > 0.15, it seems the wave transmission coefficient (C_{tn}) remains constant. It is concluded that at a small relative water depth (d/L) (long waves) the ability of the structure to absorb the wave energy is weak compared to the high relative water depth (d/L). This means that a long wave may transmit a considerable percentage of wave energy into the structure’s lee side. Thus there is less chance for the wave energy to be dissipated over the porous submerged structure. It is also concluded that ArMS submerged breakwater can meet the demand of low values in wave transmission coefficients provided the structure is of considerable width (in terms of row system).

5. It was found that increases in relative structure height (d_s/d) results in a considerable reduction in the wave transmission coefficient (C_{tn}) value for the structure of 9 and 20 row systems

within the range of wave steepness considered. Optimum wave transmission coefficient (C_{tn}) value was found at relative structure height (d_s/d) = 1.55 since at this condition the top of the structure is above still water and wave propagation can be dissipated better. In fact having structure emerged to the surface is not good aesthetically even though it may reach optimum wave absorption, it is not recommended to install the structure at this conditions. Therefore selecting proper structure height and water depth ratio is also important.

6. It was found that increasing the relative wave height in terms of H_i/d will decrease the wave transmission coefficients for different row numbers. It is noteworthy to conclude that as relative wave height (H_i/d) is greater than 0.2, the wave transmission coefficient (C_{tn}) tends to be constant and it does not vary significantly for all row systems.

7. From the numerical calculation it was found that the reflection coefficients (C_{rn}) decrease as porosities (ζ_n) increase. Wave reflection coefficients (C_{rn}) do not show clear variation for 1- to 9-row systems when the porosity (ζ_n) kept constant.

7. ACKNOWLEDGEMENT

The authors are in the process of patenting the ArMS system. The authors are also deeply indebted to Dr. Armono H. D. from ITS University, Indonesia for allowing us using his licensed software.

8. REFERENCES

1. Armono H. D. and Hall K. R. (2003). Wave Transmission on Submerged Breakwater Made of Hollow Hemispherical Shape Artificial Reefs. Canadian Coastal Conference.
2. Clause G. F and Habel R. (1999). Hydrodynamic Characteristics of Under Water Filter Systems for Coastal Protection. Canadian Coastal Conference.
3. Eldina Fatimah (2007). Hydraulic Performance of an Artificial Mangrove Root System. PhD. Thesis.
4. Flow Science Inc. (1997). Flow-3D Excellent in Flow Modeling Software, Flow-3D version 8.2. *User's Manual*. Los Alamos. NM, 97.
5. Hadibah, I., Eldina F. and Abd.Wahab, A. K. (2005). Wave Energy Dissipation over Pseudo-Mangrove Roots, Innovations & Technologies in Oceanography for Sustainable Development. *Proceedings of the 2005 ITOS Innovations and Tech nologies in Oceanography for Sustainable Development*. September 26-29. Kuala Lumpur, Malaysia. ITOS 2005: 193-204.
6. Hutchinson, P. S. and Raudkivi, A. J. (1984). Case history of a Spaced Pile Breakwater at Halfmoon Bay Marina, Auckland, New-Zealand. *Proceedings of 19th Coastal Engineering Conference, Houston, Texas*. Sept. 3-7. New York, N. Y.: ASCE: 2530-2535.
7. Madsen O. S. (1974). Wave Transmission through Porous Structures. Journal of the Waterways Harbors and Coastal Engineering Division, August 100, No. WWW3:169-186.
8. Twu, S. W. and Chieu, C. C. (2000). A highly Wave Dissipation Offshore Breakwater. *Ocean Engineering*. 27: 315-330
9. Wang K. and Williams. (2003). Flexible Porous Wave Barrier for Enhanced Wetlands Habitat Restoration. Journal of Engineering Mechanics. Vol. 129. No. 1:1-8.